Original Article

Systematic lymphatic abnormality-related osseous lesions: a study based on CT lymphangiography

Yan Zhang[1#], Xiaoli Sun[1#], Wenbin Shen[2], Kun Hao[2], Qi Hao[3], Xingpeng Li[1], Rengui Wang[1]

[1]Department of Radiology, Beijing Shijitan Hospital, Capital Medical University, Beijing, China; [2]Department of Lymph Surgery, Beijing Shijitan Hospital, Capital Medical University, Beijing, China; [3]Department of Radiology, Beijing Shijitan Hospital, Peking University Ninth School of Clinical Medicine, Beijing, China

Contributions: (I) Conception and design: Y Zhang, X Sun, R Wang; (II) Administrative support: W Shen, K Hao, R Wang; (III) Provision of study materials or patients: Y Zhang; (IV) Collection and assembly of data: Y Zhang, X Sun; (V) Data analysis and interpretation: Y Zhang, X Sun, Q Hao, X Li; (VI) Manuscript writing: All authors; (VII) Final approval of manuscript: All authors.

[#]These authors contributed equally to this work and should be considered as co-first authors.

Correspondence to: Rengui Wang. Department of Radiology, Beijing Shijitan Hospital, Capital Medical University, 10 Yangfangdian Tieyi Road, Haidian District, Beijing 100038, China. Email: wangrg@bjsjth.cn.

Background: Few studies have focused on the morphology of systematic lymphatic abnormality-related osseous lesions. In this study, we classified systematic lymphatic abnormality-related osseous lesions into four types based on their morphology and density. We also discussed the imaging features of computed tomography lymphangiography (CTL) in this disease.

Methods: In this retrospective cohort study, the clinical and imaging data of 39 patients with systematic lymphatic abnormality-related osseous lesions were collected. All patients underwent computed tomography (CT) scans of the chest and abdomen after direct lymphangiography, and two experienced radiologists evaluated the CTL features of intraosseous and extraosseous lymphatic vessel abnormalities.

Results: Intraosseous osteolytic changes were observed in all 39 patients. According to the morphological density of the lesions, systematic lymphatic abnormality-related osseous lesions were classified into four types: cyst-like (76.9%), canal-like or honeycomb-like (87.2%), osteoporosis-like (41.0%), and osteosclerosis-like (20.5%), with abnormal deposits of lipiodol seen in the first two types. Enhanced CT of the thorax and abdomen was performed in 11 cases, and enhancement was not seen in any intraosseous lesions.

Conclusions: The CTL features of systematic lymphatic abnormality-related osseous lesions have specific characteristics and are often accompanied by extraosseous abnormalities, which can provide a vital imaging basis for the diagnosis and differentiation of this disease.

Keywords: Systematic lymphatic abnormality; osseous lesions; computed tomography (CT); X-ray computer; direct lymphangiography (DLG)

Submitted Dec 12, 2021. Accepted for publication Jun 13, 2022.
doi: 10.21037/qims-21-1202
View this article at: https://dx.doi.org/10.21037/qims-21-1202

Introduction

Systematic lymphatic abnormality-related osseous lesions constitute a rare disease of the lymphatic system characterized by the proliferation and expansion of lymphatic vessels causing resorption and dissolution of bone (1). The 2018 International Society for the Study of Vascular Anomalies renamed lymphangioma as lymphatic malformations (LM) and classified it into common

(cystic) LM, generalized lymphatic anomaly, kaposiform lymphangiomatosis, LM in Gorham-Stout disease, channel type LM, "acquired" progressive lymphatic anomaly, primary lymphedema, and others (2). Generalized lymphatic anomalies, kaposiform lymphangiomatosis, and LM in Gorham-Stout disease can involve the skeleton and lead to systematic lymphatic abnormality-related osseous lesions (3,4). Gorham-Stout disease shows progressive osteolysis which may eventually lead to complete absorption and loss of entire bones, also known as vanishing bone disease. On the contrary, bone involvement in generalized lymphatic anomalies progresses slowly, and osteolysis is confined to the medulla (5-7). There are no lymphatic vessels in normal bone, and the mechanisms and triggers of lymphatic vessel endothelial cell invasion into normal bone are unknown. Lymphatic vascular epithelial cells have been shown to proliferate outside the bone, such as in the periosteum, extraosseous connective tissue, joint capsule, and synovium, and gradually invade bone tissue after breaking through the periosteum (8-10).

Direct lymphangiography (DLG) is an imaging technique in which a contrast agent is injected directly into lymphatic vessels to visualize them under X-ray. This method can provide a more intuitive picture of the lymphatic system and show the lymphatic vascular pathways throughout the body (11). A computed tomography lymphangiography (CTL) is performed a certain time after DLG, and due to the high spatial resolution of CT and powerful image postprocessing technology, the location and quantity of contrast agents deposited in the body can be displayed accurately. Tortuous dilatation and reflux of lymphatic vessels can be shown more accurately and carefully, which is an essential reference value for diagnosing and evaluating the site and degree of lesions (12,13). In addition, DLG can detect other comorbidities, such as abnormalities of lymphatic vessels in the chest and substantiality organs of the abdominopelvic cavity or soft tissue.

To our knowledge, there has been no large sample study on the CTL manifestation of systematic lymphatic abnormality-related osseous lesions. Therefore, this study aimed to improve the understanding of this disease by retrospectively analyzing the manifestation of 39 patients with the disease. We present the following article in accordance with the STROBE reporting checklist (available at https://qims.amegroups.com/article/view/10.21037/qims-21-1202/rc).

Methods

Patients

The study was conducted in accordance with the Declaration of Helsinki (as revised in 2013). The study was approved by the Ethics Committee of Beijing Shijitan Hospital, Capital Medical University, and informed consent was waived due to the retrospective nature of the study. Between January 2018 and December 2020, the clinical and imaging data of 39 patients (18 males and 21 females) diagnosed with systematic lymphatic abnormality-related osseous lesions were retrospectively reviewed at Beijing Shijitan Hospital, Capital Medical University. A total of 24 patients with generalized lymphatic anomalies and 15 patients with LM in Gorham-Stout disease were evaluated. The inclusion criteria were as follows: (I) systematic lymphatic abnormality-related osseous lesions diagnosed by a combination of clinical, radiological, and histological findings; and (II) DLG and CTL were performed. The exclusion criteria were as follows: (I) bone tumors, osteomyelitis, bone tuberculosis, and metabolic diseases such as brown tumors; and (II) DLG and CTL were not performed (*Figure 1*).

The age at diagnosis ranged from 1 to 62 years, with a mean of 19.82±15.86 years, and the duration of the disease ranged from 1 month to 24 years. The clinical manifestations of cases are shown in *Table 1*. Biopsy evidenced disease was seen in 13/39 cases, 16 had follow up imaging 2–111 months later, and five patients showed evidence of progressive disease.

DLG and CTL

A total of 39 cases underwent DLG followed by plain CT scans, and 11 underwent CT-enhanced scans of the chest and abdomen.

The DLG was performed using a GE Innova 2000-IQ DSA machine (AXIOM; Siemens Healthineers, Erlangen, Germany). The skin and subcutaneous area between the 1st and 2nd and 2nd and 3rd toes of the healthy or less edematous side of the foot were punctured and injected with 2 mL of methylene blue stain (2.5% Patent Blue V dye; 1 mL Guerbet Laboratories, Aulnay-sous-Bois, France) mixed with 2% lidocaine 1:1. Superficial lymphatic vessels were found under microscope, and ultraliquid iodized oil (Lipiodol UF, Guerbet, France) was injected with a fine

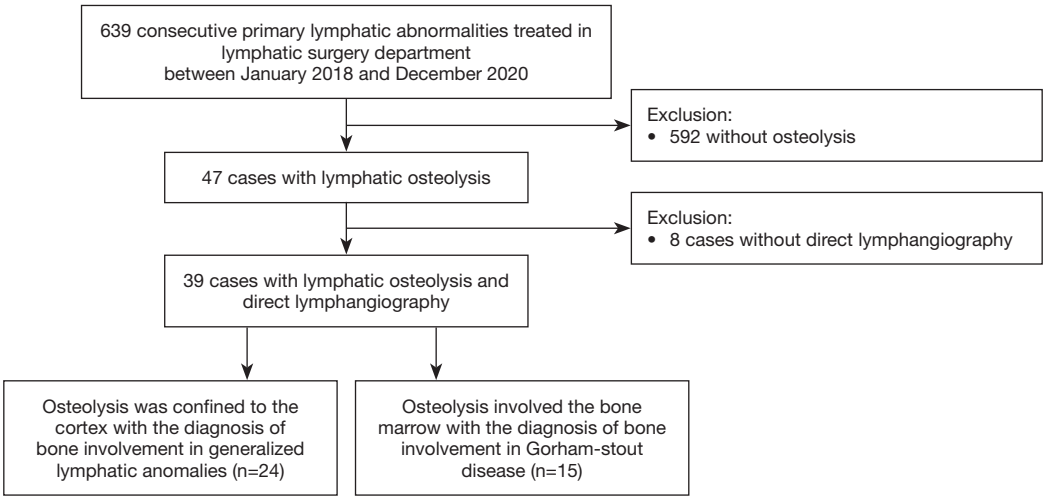

Figure 1 Study flowchart and exclusions.

Table 1 Primary clinical features of the 39 patients with systematic lymphatic abnormality-related osseous lesions

Characteristic or symptom	Cases	Proportion
Gender		
Male patients	18/39	46.2%
Female patients	21/39	53.8%
Fever	8/39	20.5%
Chest tightness	13/39	33.3%
Cough	8/39	20.5%
Abdominal pain and distension	5/39	12.8%
Diarrhea	1/39	2.6%
Bone pain	2/39	5.1%
Lumbago	3/39	7.7%
Chyluria	2/39	5.1%
Chyloptysis	1/39	2.6%
Primary limb swelling	8/39	20.5%

needle puncture of 8–20 mL. The DLG was terminated when (I) the patient breathed calmly or deeply when the contrast agent was visible in the blood from the left neck (thoracic duct) or right neck (right lymphatic duct), and sufficient lipiodol was observed in the groin at the injection site, and (II) lipiodol could not enter the thoracic duct or the right lymphatic duct as it moved cephalad but was visible in the peripheral blood vessels. In this route, due to the lack of hydrostatic pressure from the large vessels of the jugular vein, the lipiodol enters the bloodstream rapidly, and excessive amounts can lead to pulmonary embolism, requiring cessation of the procedure.

All cases were examined by unenhanced thoracic and abdominal CT scans for 30 min to 2 h on a Siemens SOMATOM Sensation 16 (Somatom Sensation Cardiac 16, Siemens Healthcare) or Philips iCT (Brilliance iCT, Philips Medical Health care, Best, the Netherlands). The CT scan ranged from the level of the inferior border of the thyroid cartilage in the neck to the inferior border of the pubic symphysis, and scan parameters were set as follows: tube voltage of 80–120 kV, tube current of 250–300 mA, and pitch of 1. After scanning, the raw data were transferred to the workstation for thin-layer reconstruction with a layer thickness of 2 mm and a layer spacing of 2 mm.

The contrast agent ioversol (Guerbet Laboratories, Villepinte, France, 320 mg/mL, 80–100 mL) was used to perform CT-enhanced scans of the chest and abdomen, and was administered by bolus injection at a flow rate of 2–4 mL/s. A three-phase enhanced CT scan was performed, and after scanning, the raw data were transferred to the CT postprocessing workstation for postprocessing reconstruction, such as multiplanar reformation (MPR), maximum intensity projection (MIP), and volume rendering (VR).

Image analysis

Two radiologists with more than 10 years of experience

Table 2 CTL features of bone lesions in 39 patients with systematic lymphatic abnormality-related osseous lesions

Lesions site	Cases	Proportion
Vertebra	39/39	100%
Cervical vertebra	10/39	25.6%
Thoracic vertebra	28/39	71.8%
Lumbar vertebra	32/39	82.1%
Sacral vertebra	29/39	74.4%
Pelvis	38/39	97.4%
Ilium	37/38	97.4%
Ischium	20/38	52.6%
Pubis	17/38	44.7%
Clavicle	7/39	17.9%
Sternum	17/39	43.6%
Scapula	19/39	48.7%
Rib	21/39	53.8%
Limb bone	24/39	61.5%
Pathological fracture	12/39	30.8%
Thoracic collapse	7/12	58.3%
Pelvic collapse	3/12	25%
Vertebral compression fracture	3/12	25%

CTL, computed tomography lymphangiography.

evaluated the following features of intra- and extraosseous lymphatic vessel abnormalities: (I) the location, size, number, morphology, margins, density, and abnormal distribution of lipiodol of intraosseous lesions; (II) abnormal lymphatic vessels of extraosseous lesions, including the location, size, density, lymphatic fluid reflux of cystic lesions, and abnormal distribution of lipiodol at other sites. A consensus was reached under the guidance of a senior physician in cases of inconsistent observations.

Results

The involvement locations and incidence of bone lesions in 39 cases are detailed in *Table 2*. According to the morphology of bone lesions, these were divided into the following four types: (I) cystic changes (n=30; *Figure 2*), which showed single or multiple round-like cystic hypodense shadows in bone. The lesions had clear borders with or without sclerotic margins, and the maximum diameter was less than 5 cm. Marginal sclerotic margins (n=28), with one case showing iodized oil deposits within the lesion. (II) canal-like or honeycomb-like changes (n=34; *Figure 3*), which showed a tortuous, tubular distribution of hypointense shadow with clear margins and continuous at multiple levels above and below. The bone cortex was smooth or irregularly fractured in a worm-like pattern, while lesions were seen in 20 cases with iodized oil deposits. (III) Osteoporosis-like changes (n=16 cases; *Figure 4*), which showed a diffuse decrease in bone density and thinning of bone trabeculae. No lipiodol deposition was seen in any of the 16 cases in this group. (IV) Osteosclerosis-like changes (n=8; *Figure 5*), with two cases showing smooth thickening of the bone cortex, three cases showing increased density of osteophytes in the medullary cavity, three cases showing mixed presence, and five cases showing narrowing of the medullary cavity. Iodized oil deposition was not observed in any case.

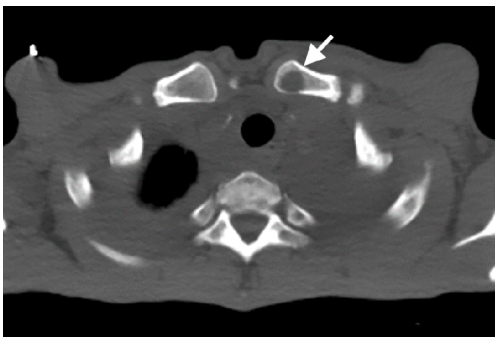

Figure 2 A 48-year-old woman with systematic lymphatic abnormality-related osseous lesions. Axial CT of the chest showed a round-like cystic hypodense shadow of the left clavicle with clear margins and no sclerotic border (white short arrow). CT, computed tomography.

A total of 11 cases underwent CT-enhanced scans of the chest and abdomen, and no enhancement was seen in any of the osseous lesions. The extraosseous lesions of 39 cases are shown in *Table 3*, *Figures 6*,7, and the abnormal distribution of lipiodol in different extraosseous areas in CTL are shown in *Table 4*, *Figure 7D*, and *Figure 8*.

Biopsies at different locations were performed in 13 cases, with three biopsies of cervical lesions, one of pulmonary lesions, one of pleural lesions, two of chest wall lesions, one of mediastinal lesions, one of mesenteric lesions, one of splenic lesions, two of retroperitoneal lesions, one of inguinal lesions, and one of perineal lesions. Pathology showed irregularly dilated, malformed lymphatic vessels in

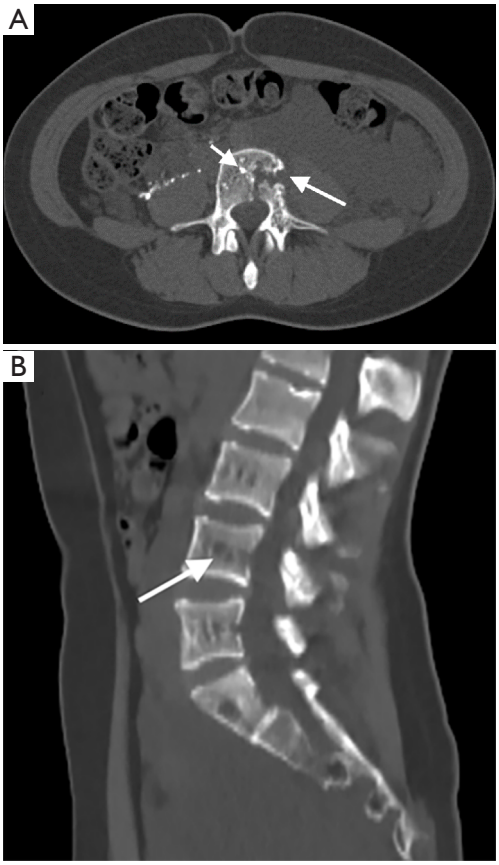

Figure 3 A 25-year-old woman with systematic lymphatic abnormality-related osseous lesions. (A) Axial CTL showing a tortuous tubular hypointense shadow (white long arrow) in the 4th lumbar vertebra with multiple abnormal distribution of lipiodol (white short arrow). (B) Sagittal CTL showing a tortuous tubular hypointense shadow in the 4th lumbar vertebral body (white long arrow). CTL, computed tomography lymphangiography.

the lesions, with some lumens interfacing with each other. Smooth muscle hyperplasia around the lumen and focal lymphocyte aggregates were also observed. All cases were diagnosed with systematic lymphatic abnormality-related osseous lesions by clinical, radiological, and histological combination.

Discussion

Systematic lymphatic abnormality-related osseous lesions are very rare and are mostly reported as single cases (14,15). Lesions can occur at any age, mostly in adolescents, with no

Figure 4 A 25-year-old woman with systematic lymphatic abnormality-related osseous lesions. Sagittal CT scan of the abdominopelvic region showing diffuse hypodensity of bone in the vertebral body of the thoracolumbar spine with sparse trabeculae (white arrow head). CT, computed tomography.

Figure 5 A 27-year-old man with systematic lymphatic abnormality-related osseous lesions. Axial CT of the pelvis showing bilateral iliac bone cortical thickening and sclerosis, narrowing of the medullary cavity, and a cystic hypodense shadow in the right iliac bone (black long arrow). CT, computed tomography.

Table 3 CTL features of extraosseous abnormalities in 39 patients with systematic lymphatic abnormality-related osseous lesions

Features of extraosseous abnormalities	Cases	Proportion
Cystic lesions	29/39	74.4%
Neck	6/29	20.7%
Chest	17/29	58.6%
Spleen	18/29	62.1%
Retroperitoneum	12/29	41.4%
Small intestine wall thickening	1/39	2.6%
Ground glass opacity and/or interlobular septal thickening in the lung	9/39	23.1%
Pleural effusion	21/39	53.8%
Peritoneal effusion	10/39	25.6%
Pericardial effusion	3/39	7.7%

CTL, computed tomography lymphangiography.

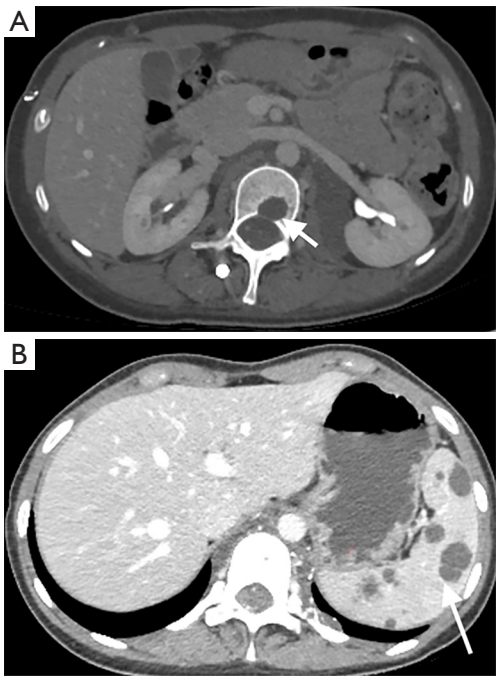

Figure 6 A 23-year-old woman with systematic lymphatic abnormality related osseous lesions. (A) Axial enhanced CT of abdomen showing round-like hypodensity of the second lumbar vertebra and no enhancement on enhanced scan (short white arrow). (B) Axial enhanced CT of abdomen showing an enlarged spleen with multiple round-like cystic shadows of different sizes with clear margins, edge enhancement on enhancement scan, and no enhancement in cystic cavity (long white arrow). CT, computed tomography.

gender differences. The male-to-female ratio in this study was approximately 1:1, and the mean age of the patients was 19.82±15.86 years, which is older than that previously reported. The disease progresses slowly (16,17), and in this study, 16 cases were reexamined on CT from 2 months to 9 years and 3 months after diagnosis, and only five had an increase in the size or number of lesions. The clinical symptoms of this disease are atypical, and most patients are not seen for symptoms of the lesioned bone itself, but rather for extraosseous symptoms (18). In our group, 35 cases were seen for clinical signs due to extraosseous lesions, and four were seen for bone pain or neurological symptoms when the lesions involved the spine.

Although pathology is the gold standard for diagnosing systematic lymphatic abnormality-related osseous lesions, pathological diagnosis often requires large bone specimens. However, it is often difficult to obtain satisfactory pathological results clinically due to the sampling method, location, and tissue volume. The diagnosis is usually a combination of clinical, radiological, and pathological diagnoses, and the former two are more critical (4,19). Imaging can clarify the location, extent, and type of lesions (11,19-21). According to Lala, Steiner, and Winterberger *et al.* (16,22,23), systematic lymphatic abnormality-related osseous lesions can occur in all body bones, with common sites of involvement the tibia, humerus, ilium, and spinal bones, and rarely in the skull. The prevalent sites in this study differed slightly from the literature, with the most common being the spinal and pelvic bones, followed by the bones of the extremities, ribs, scapulae, and sternum, although this may be because the scans were mostly confined to the thoracic and abdominal regions or to sites where clinical symptoms were present. Lesions may involve a single part of the bone or may be distributed in multiple or jump-like patterns across joints and are predominantly cancellous but can also be cortical or mixed. In the present study, all patients had lesions involving cancellous bone, including two cases with cortical sclerosis and 19 with irregular worm-like interruption of the bone cortex.

Previous literature has reported the CT manifestations of systematic lymphatic abnormality-related osseous lesions include the following (4,23): (I) osteolytic lesions in the medulla and cortex with visible or invisible sclerotic margins; (II) no periosteal reaction in the lesioned bone; (III) no vascular penetration within the lesion; and (IV)

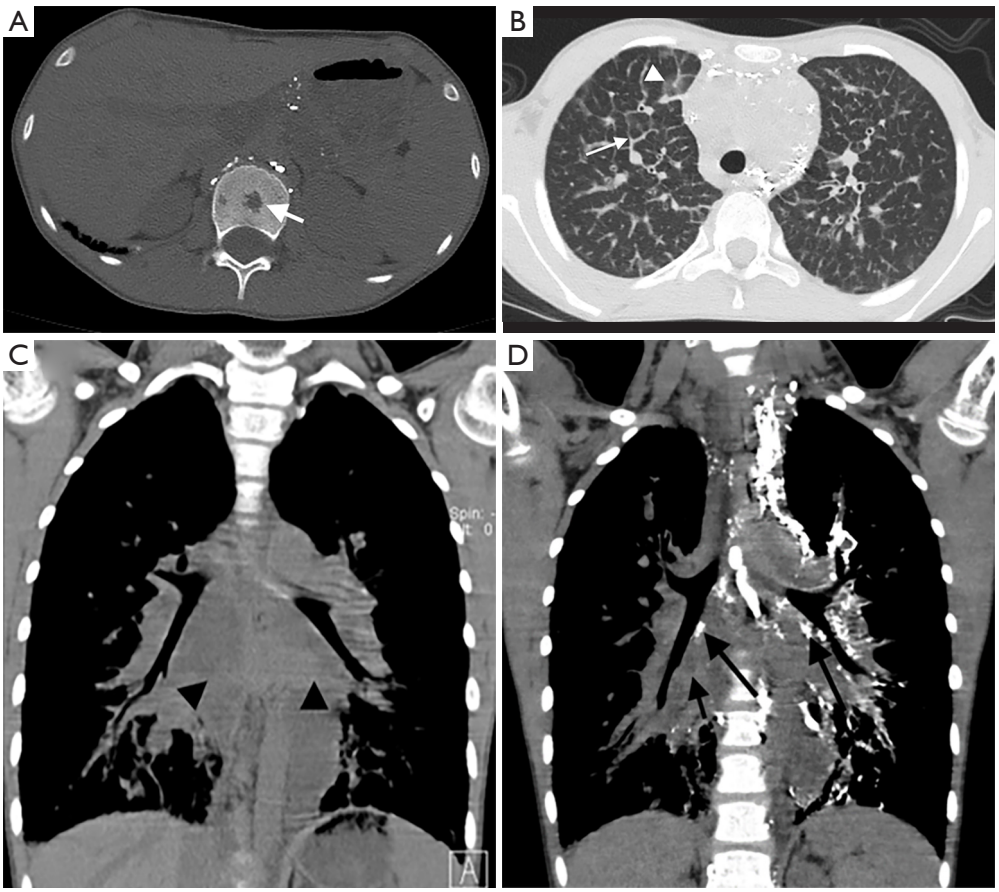

Figure 7 A 9-year-old male with systematic lymphatic abnormality-related osseous lesions. (A) Axial CTL showing the first lumbar vertebra with round-like hypodensity (white short arrow). (B) Lung window shows thickened lobular septa in both lungs (white long arrow), and scattered patchy ground glass opacity is seen (white arrow head). (C) Coronal CT of mediastinal window showing diffuse thickening of the mediastinal soft tissue (black arrow head). (D) Coronal CTL of mediastinal window showing thickened mediastinal soft tissue (black short arrow) with poor demarcation and abnormal distribution of lipiodol around bilateral pulmonary hilar and bronchial vascular bundles (black long arrow). CTL, computed tomography lymphangiography; CT, computed tomography.

swelling of the soft tissue adjacent to the affected bone but no soft tissue mass formation. All 39 cases had lesions involving cancellous bone with or without sclerotic margins in this study, and no periosteal reaction was seen. No enhancement within the lesions on enhanced CT was seen in 11 cases, which could exclude vascular-related lesions, and 25 patients had extraosseous soft tissue hyperplasia and swelling, which is consistent with literature reports. Lipiodol deposition within the lesions shown in CTL is a characteristic manifestation of systematic lymphatic abnormality-related osseous lesions, which has not been reported in the literature. In this study, based on the density and morphological characteristics of the lesions, four types of systematic lymphatic abnormality-related osseous lesions were classified: cyst-like, duct-like or honeycomb-like, osteoporosis-like, and osteosclerosis-like. Among them, lipiodol deposits were seen in only one of the lesions with cystic changes, which was considered because: (I) the lesion did not communicate with the lymphatic vessels; (II) the waiting time after direct lymphangiography was short, and lipiodol had not yet entered the lesion. The extraosseous manifestations of CTL are suggestive for the diagnosis of systematic lymphatic abnormality-related osseous lesions. In our study, extraosseous lymphatic abnormalities were seen in all 39 patients, including lymphangiectasia, celiac disease, small bowel lymphangiectasia, and abnormal distribution and reflux of lipiodol in various extraosseous sites.

There is no gold standard for treating this disease, and

Table 4 Abnormal distribution of extraosseous lipiodol in CTL in 39 patients with systematic lymphatic abnormality-related osseous lesions

Abnormal distribution of lipiodol	Cases	Proportion
Soft tissue around the bone	22/39	56.4%
Thoracic duct	26/39	66.7%
Neck	5/39	12.8%
Right side	2/5	40.0%
Left side	3/5	60.0%
Supraclavicular region	17/39	43.6%
Left side	11/17	64.7%
Bilateral sides	6/17	35.3%
Infraclavicular region	16/39	41.0%
Right side	1/16	6.2%
Left side	10/16	62.5%
Bilateral sides	5/16	31.3%
Axilla	8/39	20.5%
Right side	5/8	62.5%
Left side	3/8	37.5%
Mediastinum	14/39	35.9%
Pericardium	5/39	12.8%
Intercostal region	10/39	25.6%
Right side	6/10	60%
Left side	3/10	30%
Bilateral sides	1/10	10%
Soft tissues on both sides of the spine	8/39	20.5%
Pleural cavity	12/39	30.8%
Right side	5/12	41.7%
Left side	4/12	33.3%
Bilateral sides	3/12	25%
Lung	3/39	7.7%
Right side	1/3	33.3%
Left side	2/3	66.7%
Iliac reflux	20/39	51.3%
Inguinal reflux	10/39	25.6%
Retroperitoneum	17/39	43.6%
Perineum	8/39	20.5%
Perienteric region	3/39	7.7%
Hepatic hilus	3/39	7.7%
Splenic hilus	1/39	2.6%
Renal sinus	2/39	5.1%
Left side	1/2	50%
Bilateral sides	1/2	50%
Perirenal region	2/39	5.1%
Left side	1/2	50%
Bilateral sides	1/2	50%

CTL, computed tomography lymphangiography.

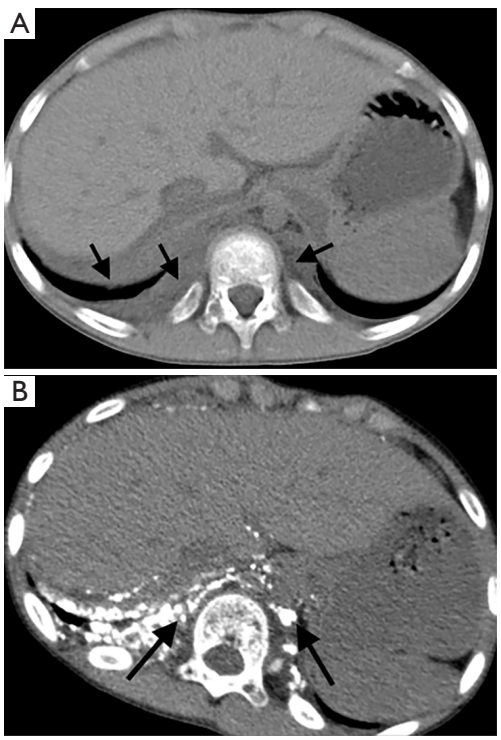

Figure 8 An 8-year-old female with systematic lymphatic abnormality related osseous lesions. (A) Axial CT showing soft tissue thickening on both sides of the spine (black short arrow). (B) Axial CTL showing multiple abnormal distribution of lipiodol on both sides of the spine (black long arrow). CTL, computed tomography lymphangiography; CT, computed tomography.

treatment varies according to the severity and location. Treatment includes drugs (e.g., sirolimus, trametinib, INF-α2b, bisphosphonates) (5,24-26), surgery, radiotherapy, chemotherapy, and combination therapy (1,27). Different treatment methods have their own advantages, and individualized treatment schemes can be formulated according to the individual circumstances of patients (1). Although the prognosis is varied and challenging to predict, younger age and patients with chest symptoms, such as chylothorax and pericardial effusion, seem to have a poorer prognosis (5,25,28).

There were some limitations to our study. Firstly, this was a retrospective study, and as the scan covered the thoracic and abdominal areas or areas where clinical symptoms were present; other areas may have been overlooked. Secondly, all cases in this study were diagnosed as systematic lymphatic abnormality-related osseous lesions by a combination of clinical, radiological, and pathological tests, 13 of which were puncture biopsies, and the puncture sites were not at the lesioned bones. Therefore, a controlled study of pathology and imaging at the lesion bone was not performed.

In conclusion, systematic lymphatic abnormality-related osseous lesions is a rare lymphatic disease with multiorgan involvement. A CTL can provide critical diagnostic information in showing lymphatic abnormalities and provides a vital imaging basis for diagnosing and differentiating the disease.

Acknowledgments

Funding: The work was supported by the National Natural Science Foundation of China (No. 61876216) and Beijing Shijitan Hospital, Capital Medical University (No. 2020-q18).

Footnote

Reporting Checklist: The authors have completed the STROBE reporting checklist. Available at https://qims.amegroups.com/article/view/10.21037/qims-21-1202/rc

Conflicts of Interest: All authors have completed the ICMJE uniform disclosure form (available at https://qims.amegroups.com/article/view/10.21037/qims-21-1202/coif). The authors have no conflicts of interest to declare.

Ethical Statement: The authors are accountable for all aspects of the work in ensuring that questions related to the accuracy or integrity of any part of the work are appropriately investigated and resolved. The study was conducted in accordance with the Declaration of Helsinki (as revised in 2013). The study was approved by the Ethics Committee of Beijing Shijitan Hospital, Capital Medical University, and informed consent was waived due to the retrospective nature of the study.

References

1. Rössler J, Saueressig U, Kayser G, von Winterfeld M, Klement GL. Personalized Therapy for Generalized Lymphatic Anomaly/Gorham-Stout Disease With a Combination of Sunitinib and Taxol. J Pediatr Hematol Oncol 2015;37:e481-5.
2. Monroe EJ. Brief Description of ISSVA Classification for Radiologists. Tech Vasc Interv Radiol 2019;22:100628.
3. Wassef M, Blei F, Adams D, Alomari A, Baselga E, Berenstein A, Burrows P, Frieden IJ, Garzon MC, Lopez-Gutierrez JC, Lord DJ, Mitchel S, Powell J, Prendiville J, Vikkula M; ISSVA Board and Scientific Committee. Vascular Anomalies Classification: Recommendations From the International Society for the Study of Vascular Anomalies. Pediatrics 2015;136:e203-14.
4. Ricci KW, Iacobas I. How we approach the diagnosis and management of complex lymphatic anomalies. Pediatr Blood Cancer 2021. [Epub ahead of print].
5. Ricci KW, Hammill AM, Mobberley-Schuman P, Nelson SC, Blatt J, Bender JLG, McCuaig CC, Synakiewicz A, Frieden IJ, Adams DM. Efficacy of systemic sirolimus in the treatment of generalized lymphatic anomaly and Gorham-Stout disease. Pediatr Blood Cancer 2019;66:e27614.
6. Iacobas I, Adams DM, Pimpalwar S, Phung T, Blei F, Burrows P, Lopez-Gutierrez JC, Levine MA, Trenor CC 3rd. Multidisciplinary guidelines for initial evaluation of complicated lymphatic anomalies-expert opinion

consensus. Pediatr Blood Cancer 2020;67:e28036.
7. Le HDT, Vo DS, Le DD, Dang CT, Nguyen Thanh T. Generalized lymphangiomatosis-A rare manifestation of lymphatic malformation. Radiol Case Rep 2020;16:66-71.
8. Ozeki M, Fukao T. Generalized Lymphatic Anomaly and Gorham-Stout Disease: Overview and Recent Insights. Adv Wound Care (New Rochelle) 2019;8:230-45.
9. Monroy M, McCarter AL, Hominick D, Cassidy N, Dellinger MT. Lymphatics in bone arise from pre-existing lymphatics. Development 2020;147:dev184291.
10. Edwards JR, Williams K, Kindblom LG, Meis-Kindblom JM, Hogendoorn PC, Hughes D, Forsyth RG, Jackson D, Athanasou NA. Lymphatics and bone. Hum Pathol 2008;39:49-55.
11. Jin D, Sun X, Shen W, Zhao Q, Wang R. Diagnosis of Lymphangiomatosis: A Study Based on CT Lymphangiography. Acad Radiol 2020;27:219-26.
12. Sun X, Shen W, Chen X, Wen T, Duan Y, Wang R. Primary intestinal lymphangiectasia: Multiple detector computed tomography findings after direct lymphangiography. J Med Imaging Radiat Oncol 2017;61:607-13.
13. Zhang C, Chen X, Wen T, Zhang Q, Huo M, Dong J, Shen WB, Wang R. Computed tomography lymphangiography findings in 27 cases of lymphangioleiomyomatosis. Acta Radiol 2017;58:1342-8.
14. Fattahi A, Taheri M, Majdi M. Lymphangioma of the Thoracic Spine with Epidural Compression: A Case Report. Iran J Med Sci 2019;44:172-5.
15. Aslan F, Güvenç İ, Aslan A, Günaydın E. Cystic Hygroma with Multiple Benign Bone Lymphangiomas in an Adult Patient: A Rare Entity in the Differential Diagnosis of Multiple Osseous Lesions in Oncology Practice. Curr Med Imaging 2021;17:439-42.
16. Lala S, Mulliken JB, Alomari AI, Fishman SJ, Kozakewich HP, Chaudry G. Gorham-Stout disease and generalized lymphatic anomaly--clinical, radiologic, and histologic differentiation. Skeletal Radiol 2013;42:917-24.
17. Martinat P, Cotten A, Singer B, Petyt L, Chastanet P. Solitary cystic lymphangioma. Skeletal Radiol 1995;24:556-8.
18. Lopez-Gutierrez JC, Miguel M, Diaz M, Ros Z, Tovar JA. Osteolysis and lymphatic anomalies: a review of 54 consecutive cases. Lymphat Res Biol 2012;10:164-72.
19. Beveridge N, Allen L, Rogers K. Lymphoscintigraphy in the diagnosis of lymphangiomatosis. Clin Nucl Med 2010;35:579-82.
20. Wunderbaldinger P, Paya K, Partik B, Turetschek K, Hörmann M, Horcher E, Bankier AA. CT and MR imaging of generalized cystic lymphangiomatosis in pediatric patients. AJR Am J Roentgenol 2000;174:827-32.
21. Charruau L, Parrens M, Jougon J, Montaudon M, Blachère H, Latrabe V, Laurent F. Mediastinal lymphangioma in adults: CT and MR imaging features. Eur Radiol 2000;10:1310-4.
22. Steiner GM, Farman J, Lawson JP. Lymphangiomatosis of bone. Radiology 1969;93:1093-8.
23. Winterberger AR. Radiographic diagnosis of lymphangiomatosis of bone. Radiology 1972;102:321-4.
24. Homayun-Sepehr N, McCarter AL, Helaers R, Galant C, Boon LM, Brouillard P, Vikkula M, Dellinger MT. KRAS-driven model of Gorham-Stout disease effectively treated with trametinib. JCI Insight 2021;6:149831.
25. Ramaroli DA, Cavarzere P, Cheli M, Provenzi M, Barillari M, Rodella G, Gaudino R, Antoniazzi F. A Child with Early-Onset Gorham-Stout Disease Complicated by Chylothorax: Near-Complete Regression of Bone Lesions with Interferon and Bisphosphonate Treatment. Horm Res Paediatr 2019;91:406-10.
26. Schneider KN, Masthoff M, Gosheger G, Klingebiel S, Schorn D, Röder J, Vogler T, Wildgruber M, Andreou D. Gorham-Stout disease: good results of bisphosphonate treatment in 6 of 7 patients. Acta Orthop 2020;91:209-14.
27. Ozeki M, Fujino A, Matsuoka K, Nosaka S, Kuroda T, Fukao T. Clinical Features and Prognosis of Generalized Lymphatic Anomaly, Kaposiform Lymphangiomatosis, and Gorham-Stout Disease. Pediatr Blood Cancer 2016;63:832-8.
28. Ludwig KF, Slone T, Cederberg KB, Silva AT, Dellinger M. A New Case and Review of Chylothorax in Generalized Lymphatic Anomaly and Gorham-Stout Disease. Lymphology 2016;49:73-84.

Cite this article as: Zhang Y, Sun X, Shen W, Hao K, Hao Q, Li X, Wang R. Systematic lymphatic abnormality-related osseous lesions: a study based on CT lymphangiography. Quant Imaging Med Surg 2022;12(9):4549-4558. doi: 10.21037/qims-21-1202

